DYNAMIC PROPERTIES AND CHAOTIC PHENOMENA IN CONCATENATION MODEL WITH POWER-LAW NONLINEARITY WITH EXTERNAL PERTURBATION TERMS

Bing Guan [a,b], Xianjun Wang [c], Xiaofei Fu [a]
Shuangqing Chen [d,†]

[a]Key Laboratory of Continental Shale Hydrocarbon Accumulation and Efficient Development, Northeast Petroleum University
Daqing 163318, China
[b]Postdoctoral Programme of Daqing Oilfield, Daqing 163318, China
[c]Daqing Oilfield Co., Ltd. Oil Production Technology Research Institute
Daqing 163318, China
[d]School of Petroleum Engineering
Northeast Petroleum University, Daqing 163318, China

Received 31 March 2025, accepted 3 July 2025,
published online 16 July 2025

This paper presents an in-depth study of a concatenation model with power-law nonlinearity. The integral form of the original model is derived, and the corresponding dynamic system is obtained. A qualitative analysis is conducted to identify the types of equilibrium points, phase diagrams, and trajectories. From specific trajectories, we can infer that this equation has periodic and soliton solutions. To validate these conclusions, the corresponding exact solutions are constructed, and several new solutions are initially presented in this paper. Finally, by adding a specific external perturbation term, we found that this model also exhibits chaotic behavior, which is presented in this paper for the first time.

DOI:10.5506/APhysPolB.56.7-A4

1. Introduction

The concatenation model is an innovative approach in the study of pulse propagation dynamics in optical fibers [1–3] that integrates three well-established nonlinear evolution equations: the nonlinear Schrödinger equation, the Sasa–Satsuma equation, and the Lakshmanan–Porsezian–Daniel model. This model effectively describes the behavior of long-distance optical solitons and has been studied extensively from different perspectives.

† Corresponding author: `csqing2590@163.com`

These include its historical connection to Painlevé analysis, numerical analysis using the Laplace–Adomian decomposition method for the identification of conservation laws, the study of stable solitons in the presence of nonlinear chromatic dispersion (CD) effects, and various other findings [4–8]. The previous analysis was conducted within the framework of Kerr nonlinearity, which describes the empirical relationship between refractive index change and light intensity as light propagates through a medium [9, 10]. A specific manifestation of the Kerr effect in optical pulse transmission is a self-phase modulation (SPM). This paper extends the concept of SPM to power-law nonlinearity, allowing for a power-law relationship between the nonlinear response and optical intensity, rather than the conventional linear or cubic relationship. The concatenation model with the power-law nonlinearity represents a significant advancement in the study of pulse propagation dynamics in optical fibers. The power-law nonlinearity manifests in diverse physical phenomena, including light propagation in nonlinear optical media, Bose–Einstein condensate dynamics, and other systems exhibiting nonlinear responses. Thus, the research on the concatenation model with the power-law nonlinearity is of great significance for governing and analyzing optical propagation phenomena. The concatenation model with the power-law nonlinearity is defined as in Eq. (1) [11], which is a common variant of the concatenation model

$$\begin{aligned} &iq_t + aq_{xx} + b|q|^{2n}q + c_1\left[\sigma_1 q_{xxxx} + \sigma_2(q_x)^2q^* + \sigma_3|q_x|^2q + \sigma_4|q|^{2n}q_{xx}\right. \\ &\left.+\sigma_5 q^2q_{xx}^2 + \sigma_6|q|^{2n+2}q\right] + ic_2\left[\sigma_7 q_{xxx} + \sigma_8|q|^{2n}q_x + \sigma_9 q^2q_x^*\right] = 0\,, \end{aligned} \tag{1}$$

where $q(x,t)$ denotes the wave profile and the complex-valued function, x is the spatial variable, t signifies the temporal variable, n denotes the power-law nonlinearity parameter, a is the coefficient of chromatic dispersion, b is the coefficient of the Kerr law of self-phase modulation, c_1 is the coefficient derived from the Lakshmanan–Porsezian–Daniel model, c_2 is a coefficient from the Sasa–Satsuma equation, and $\sigma_1, \sigma_2, \sigma_3, \sigma_4, \sigma_5, \sigma_6, \sigma_7, \sigma_8, \sigma_9$ are constants.

Qualitative analysis is an effective technique [12, 13] for analyzing the physical laws governing light-wave propagation. Qualitative analyses have been conducted on significant physical equations, such as the cubi–quartic nonlinear Schrödinger equation [14, 15], the Khokhlov–Zabolotskaya–Kuznetsov equation [16], and the Nagumo nerve conduction equation [17]. Analyzing chaotic behavior provides deeper insights into the underlying physical principles of optical propagation [18–20]. There are many methods for solving nonlinear partial differential equations and obtaining exact traveling wave solutions for various physical equations. These include the new Kudryashov method [21], the Lie symmetry method [22, 23], the first integral method [24, 25], the exp-function method [26, 27], *etc.* The complete discrimination system for the polynomial method [28–33] is a newly proposed method that has obtained exact solutions for many classical equations [34–40]. In this paper, the original model is transformed into an integral form using a traveling wave transformation. From this integral form, a corresponding dynamic system is derived. Through a qualitative analysis, the types of equilibrium points, phase diagrams, and trajectories are identified. In addition, the existence of solitons and periodic solutions is established by analyzing the characteristics of these trajectories. To validate the findings from the qualitative analysis, the corresponding exact solutions to the dynamic system are constructed, leading to the discovery of several new solutions. Finally, the models response to specific external perturbation terms is examined, revealing that the system can exhibit chaotic behaviors under specific conditions. In addition, the chaotic behaviors identified in this work are reported for the first time, illuminating the future study of the mechanisms underlying chaotic phenomena in nonlinear optics.

The remainder of this paper is structured as follows: Section 2 elaborates on the traveling wave reduction methodology. Section 3 conducts a qualitative analysis of the system. Section 4 derives exact traveling wave solutions for Eq. (1), while Section 5 systematically investigates the chaotic dynamics. The comprehensive findings and discussions are presented in Section 6.

2. Traveling wave reduction

By taking the following traveling wave transformation:

$$q(x,\ t) = y(\xi)\,\mathrm{e}^{i(kx-wt+\theta_0)}\,, \qquad \xi = x - vt\,, \tag{2}$$

and substituting it into Eq. (1), the resulting overdetermined system of equations can be obtained [8]. The imaginary part of the results is presented as follows:

$$\begin{aligned}&(c_2\sigma_7 + 4c_1k\sigma_1)y''' + (c_2\sigma_8 + 2c_1k\sigma_4)y^{2n}y' + (c_2\sigma_9 + 2c_1k\sigma_2 - 2c_1k\sigma_5)y^2y'\\ &+ \left(2ak - 4c_1\sigma_1k^3 - 3c_2\sigma_7k^2 - v\right)y' = 0\,.\end{aligned} \tag{3}$$

The real part of the results is presented as follows:

$$\begin{aligned}&c_1\sigma_1y^{(4)} + \left(b - c_1k^2\sigma_4 - c_2k\sigma_8\right)y^{2n+1} + c_1\sigma_6y^{2n+3} + c_1\sigma_4y^{2n}y''\\ &+ \left(a - 6c_1k^2\sigma_1 - 3c_2k\sigma_7\right)y'' + c_1\sigma_5y^2y'' + c_1(\sigma_2+\sigma_3)y\left(y'\right)^2\\ &- \left(k^2c_1\sigma_2 - c_1\sigma_3k^2 + k^2c_1\sigma_5 - k\sigma_9c_2\right)y^3\\ &- \left(ak^2 - w - \sigma_1k^4c_1 - c_2\sigma_7k^3\right)y = 0\,,\end{aligned} \tag{4}$$

where $y(\xi)$ is the envelope packet, θ_0 is a constant, k is the wave number, and w is the wave velocity. Equations (3) and (4) can be simplified into the following form:

$$\left(y'\right)^2 = Ay^4 + By^{2n+2} + Cy^2 + Dy + E\,, \tag{5}$$

where

$$\begin{aligned} A &= -\frac{c_2\sigma_8 + 2c_1k\sigma_4}{(2n+1)(n+1)(c_2\sigma_7 + 4c_1k\sigma_1)}\,, \\ B &= -\frac{c_2\sigma_9 + 2c_1k\sigma_2 - 2c_1k\sigma_5}{6(c_2\sigma_7 + 4c_1\sigma_1)}\,, \\ C &= -\frac{2ak - 4c_1k\sigma_1k^3 - 3c_2\sigma_7k^2 - v}{c_2\sigma_7 + 4v_1k\sigma_1}\,, \\ D &= \frac{2C_1}{c_2\sigma_7 + 4c_1k\sigma_1}\,, \end{aligned} \tag{6}$$

and C_1 and E are arbitrary constants. In the following equation, we focus on the condition of $n = \frac{1}{2}$:

$$\left(y'\right)^2 = Ay^4 + By^3 + Cy^2 + Dy + E\,, \tag{7}$$

and other cases could be conducted similarly. Through the following transformation:

$$\phi = A^{\frac{1}{4}}\left(y + \frac{B}{4A}\right)\,, \qquad \varsigma = A^{\frac{1}{4}}\xi\,, \tag{8}$$

we obtain the following equation:

$$(\phi_\varsigma)^2 = \phi^4 + a_2\phi^2 + a_1\phi + a_0\,, \tag{9}$$

where $a_2 = \frac{C}{\sqrt{A}}$, $a_1 = (\frac{B^3}{8A^2} - \frac{BC}{2A} + D)$, $a_0 = -\frac{-3B^4}{256A^3} + \frac{B^2C}{16A^2} - \frac{BD}{4A} + E$.

Equation (7) can be transformed into the following dynamic system:

$$\begin{aligned} \phi' &= \psi\,, \\ \psi' &= 2\left(\phi^3 + b_2\phi + b_1\right)\,, \end{aligned} \tag{10}$$

where $b_2 = \frac{1}{2}a_2$, $b_1 = \frac{1}{4}a_1$. Then, we can obtain a conserved quantity as follows:

$$H(\phi,\ \psi) = \psi^2 - \left(\phi^4 + a_2\phi^2 + a_1\phi\right) \tag{11}$$

due to the following equation:

$$\frac{\mathrm{d}H}{\mathrm{d}\varsigma} = \frac{\partial H}{\partial\phi}\frac{\partial\phi}{\partial\xi} + \frac{\partial H}{\partial\psi}\frac{\partial\psi}{\partial\xi} = 0\,. \tag{12}$$

In fact, $H(\phi,\ \psi)$ represents the Hamiltonian; thus, $-(\phi^4 + a_2\phi^2 + a_1\phi)$ corresponds to the potential energy $U(\phi)$ of the system. In addition, since Eq. (11) is autonomous, the system trajectories correspond exactly to the contour lines of the function $H(\phi,\ \psi)$. This relationship is used in the following sections to conduct the qualitative analysis.

3. Qualitative analysis

By introducing the following discriminant:

$$\Delta = -\left(\frac{b_2}{4} + \frac{b_1}{27}\right), \tag{13}$$

four cases arise that require detailed analysis.

Case 1. $\Delta = 0$, $b_2 < 0$, $U(\phi)'$ is given as follows:

$$-U(\phi)' = 4(\phi - a)(\phi - b)^2, \qquad (a + 2b = 0). \tag{14}$$

There are two equilibrium points: $(a,\ 0)$, which is a center, and $(b,\ 0)$, which is a cuspidal point. For example, when $a = 1$, $b = -0.5$, the corresponding phase diagram is shown in Fig. 1. Figures 1–4 were created by using the drawing functions of the MATLAB software.

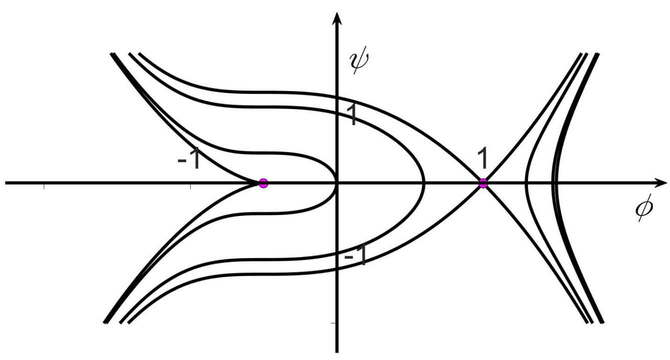

Fig. 1. Phase diagram of Case 1 when $a = 1$, $b = -0.5$.

Case 2. $\Delta = 0$, $b_2 = 0$, $U(\phi)'$ is given as follows:

$$-U(\phi)' = 4\phi^3. \tag{15}$$

There is one equilibrium point under this condition: $(0, 0)$, which is a cuspidal point. For example, when $b_1 = b_2 = 0$, this case is realized, and the corresponding phase diagram is shown in Fig. 2.

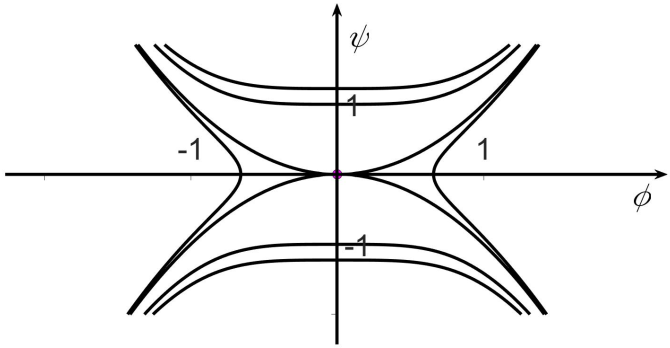

Fig. 2. Phase diagram of Case 2 when $b_1 = 0$, $b_2 = 0$.

Case 3. $\Delta > 0$, $b_2 < 0$, $U(\phi)'$ is presented as follows:

$$-U(\phi)' = 4(\phi - a)(\phi - b)(\phi - c)\,, \qquad (a + b + c = 0\,, \quad a < b < c)\,. \quad (16)$$

In this case, there are three equilibrium points: $(a,\ 0)$ and $(c,\ 0)$, which are nodes, and $(b,\ 0)$, which is a center. The value of $b = 0$ influences the topological properties of the phase diagram. For example, the conditions of $a = -0.5$, $b = 0$, $c = 0.5$ and $a = -2$, $b = -1$, $c = 3$ are shown in Figs. 3–4.

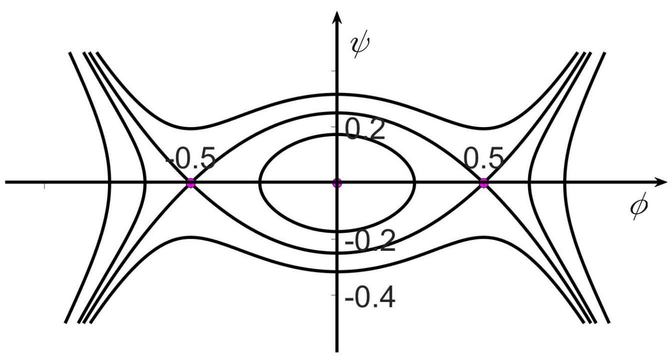

Fig. 3. Phase diagram of Case 3 when $a = -0.5$, $b = 0$, $c = 0.5$.

For the symmetric case shown in Fig. 3, there are two heteroclinic orbits, indicating the existence of kink and antikink solitary wave solutions. In addition, a closed trajectory with an interior center point is present, signifying that the original model has a periodic solution. In contrast, for the asymmetric case shown in Fig. 4, there is a homoclinic trajectory and a closed trajectory featuring an interior center point. This suggests the existence of a bell-shaped soliton solution and a periodic solution.

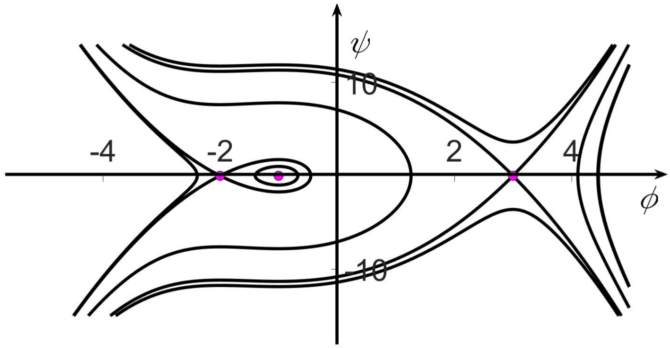

Fig. 4. Phase diagram of Case 3 when $a = -2$, $b = -1$, $c = 3$.

Case 4. $\Delta < 0$, $U(\phi)'$ is given as follows:

$$-U(\phi)' = 4(\phi - a)\left[\phi + c^2\right] . \tag{17}$$

There is one equilibrium point, $(a,\ 0)$, identified as a saddle point. Since this case is analogous to Case 1, the corresponding results can be referenced from Case 1.

In this section, we conduct a qualitative analysis of Eq. (10) and prove the existence of solitary wave, soliton, and periodic solutions. To demonstrate our conclusions more directly, we construct all the traveling wave solutions. The results show that these solutions indeed exist.

4. Classification of traveling wave solutions

By denoting $Q(\phi) = \phi^4 + a_2\phi^2 + a_1\phi + a_0$ and introducing the following discrimination system:

$$\begin{aligned} R_1 &= 4\,, \quad R_2 = -b_2\,, \quad R_3 = -2b_2^3 + 8b_2b_0 - 9b_1^2\,, \quad Z_2 = 9b_2^2 - 32b_2b_0\,, \\ R_4 &= -b_2^3b_1^2 + 4b_2^4b_0 + 36b_2b_1^2 - 32b_2^2b_0^2 - \frac{27}{4}b_1^4 + 64b_0^3\,, \end{aligned} \tag{18}$$

we can obtain nine cases of exact traveling wave solutions.

4.1. Solitary wave solutions

Case 1. For $R_4 = 0$, $R_3 = 0$, $R_2 > 0$, and $Z_2 > 0$, we have the following equation:

$$Q(\phi) = (\phi - r)^2(\phi - o)^2\,, \qquad (r + o = 0)\,, \tag{19}$$

where $r > o$. We can obtain the following equation:

$$\pm(\xi_1 - \xi_0) = \int \frac{\mathrm{d}\phi}{(\phi - r)(\phi - o)} = \frac{1}{r - o} \ln \left| \frac{\phi - r}{\phi - o} \right| . \tag{20}$$

When $\phi > r$ or $\phi < o$, the solution can be denoted as follows:

$$\phi = \frac{o - r}{\mathrm{e}^{\pm(r-o)(\xi_1 - \xi_0)} - 1} + o = \frac{o - r}{2} \left[\coth \frac{\pm(r - o)(\xi_1 - \xi_0)}{2} - 1 \right] + o \, , \tag{21}$$

and when $o < \phi < r$, we can obtain the following equation:

$$\phi = \frac{o - r}{-\mathrm{e}^{\pm(o-m)(\xi_1 - \xi_0)} - 1} + o = \frac{o - r}{2} \left[\tanh \frac{\pm(r - o)(\xi_1 - \xi_0)}{2} - 1 \right] + o \, . \tag{22}$$

Equations (21) and (22) are solitary wave solutions. Specifically, Eq. (22) represents the antikink solitary wave solution, whereas Eq. (21) represents a singular and kink solitary wave solution.

Case 2. When $R_4 = 0$ and $R_2 R_3 < 0$, we obtain the following equation:

$$Q(\phi) = (\phi - \mu)^2 \left[(\phi - r)^2 + o^2 \right] , \qquad (\mu + r = 0) \, , \tag{23}$$

where μ, r, and o are real numbers. Then, the expression can be presented as follows:

$$\begin{aligned} \pm(\xi_1 - \xi_0) &= \int \frac{\mathrm{d}\phi}{(\phi - \mu)\sqrt{(\phi - r)^2 + o^2}} \\ &= \frac{1}{\sqrt{(\mu - r)^2 + o^2}} \ln \left| \frac{\epsilon\phi + \eta - \sqrt{(\phi - r)^2 + o^2}}{\phi - \mu} \right| , \end{aligned} \tag{24}$$

where

$$\begin{aligned} \delta &= \frac{\mu - 2s}{\sqrt{(\mu - r)^2 + o^2}} \, , \\ \eta &= \sqrt{(\mu - r)^2 + o^2} - \frac{\mu(\mu - 2s)}{\sqrt{(\mu - r)^2 + o^2}} \, . \end{aligned} \tag{25}$$

Thus, the following expression can be obtained:

$$\phi = \frac{\left(\mathrm{e}^{\pm\sqrt{(\mu - r)^2 + o^2}(\xi_1 - \xi_0)} - \delta \right) + \sqrt{(\mu - r)^2 + o^2}(2 - \delta)}{\left(\mathrm{e}^{\pm\sqrt{(\mu - r)^2 + o^2}(\xi_1 - \xi_0)} - \delta \right)^2 - 1} \, . \tag{26}$$

Equation (26) is a singular solitary wave solution. Specifically, when $\delta = 0$ and $\sqrt{(\mu - r)^2 + o^2}(2 - \delta) = 1$, a bell-shaped soliton solution is obtained.

Case 3. For $R_4 = 0$, $R_3 > 0$, and $R_2 > 0$, we get

$$Q(\phi) = (\phi - \mu_1)^2(\phi - \mu_2)(\phi - \mu_3)\,, \qquad (2\mu_1 + \mu_2 + \mu_3 = 0)\,, \tag{27}$$

where $\mu_2 > \mu_3$. By setting $h = (\mu_1 - \mu_2)(\mu_1 - \mu_3)$, we have

$$\phi = \frac{2h}{\pm(\mu_2 - \mu_3)\sinh[\sqrt{-h}(\xi_1 - \xi_0)] - (2\mu_1 - \mu_2 - \mu_3)}\,, \qquad (\mu_2 > \mu_1 > \mu_3) \tag{28}$$

and

$$\phi = \frac{2h}{(\mu_2 - \mu_3)\cosh[\sqrt{h}(\xi - \xi_0)] - (2\mu_1 - \mu_2 - \mu_3)}\,, \qquad (\mu_1 > \mu_2 \text{ or } \mu_1 < \mu_3)\,. \tag{29}$$

Equations (28) and (29) are twisted soliton solutions.

4.2. Periodic solutions

The periodic solutions are presented in Cases 1 to 4.

Case 1. When $R_4 = 0$, $R_3 = 0$, and $R_2 < 0$, $Q(\phi)$ can be written as follows:

$$Q(\phi) = \left(\phi^2 + o^2\right)^2\,, \tag{30}$$

where $m > 0$. Thus, we obtain the following equation:

$$\pm(\xi_1 - \xi_0) = \int \frac{\mathrm{d}\phi}{\phi^2 + o^2} = \frac{1}{o}\arctan\frac{\phi}{o}\,. \tag{31}$$

Then, we obtain the following solution:

$$q = \pm o \tan o(\xi_1 - \xi_0)\,, \tag{32}$$

which is a triangle function periodic solution.

Case 2. When $R_4 > 0$ and $R_2 R_3 \leq 0$, we obtain the following equation:

$$Q(\phi) = \left((\phi - \mu_1)^2 + s_1^2\right)\left((\phi - \mu_2)^2 + s_2^2\right)\,, \tag{33}$$

where $l_1 \geq l_2 > 0$. By applying the following transformation:

$$\phi = \frac{R_1 \tan\theta + R_2}{R_3 \tan\theta + R_4}\,, \tag{34}$$

where

$$
\begin{aligned}
R_1 &= \mu_1 R_3 + s_1 R_4\,, \\
R_2 &= \mu_1 R_4 - s_1 R_3\,, \\
R_3 &= -s_1 - \frac{l_2}{f_2}\,, \\
R_4 &= \mu_1 - \mu_2\,, \\
e_2 &= \frac{(\mu_1-\mu_2)^2 + s_1^2 + s_2^2}{2 s_1 s_2}\,, \\
f_2 &= e_2 + \sqrt{e_2^2 - 1}\,,
\end{aligned} \tag{35}
$$

we obtain the following equation:

$$
\begin{aligned}
\xi_1 - \xi_0 &= \int \frac{\mathrm{d}\phi}{\sqrt{\left((\phi-\mu_1)^2 + s_1^2\right)\left((\phi-\mu_2)^2 + s_2^2\right)}} \\
&= \frac{R_3^2 + R_4^2}{s_2\sqrt{\left(R_3^2+R_4^2\right)\left(f_2^2 R_3^2 + R_4^2\right)}} \int \frac{\mathrm{d}\theta}{\sqrt{r - m_2^2 \sin^2\theta}}\,,
\end{aligned} \tag{36}
$$

where $m_2^2 = \frac{f_2^2-1}{f_2^2}$. Then, the solution can be presented as follows:

$$
\phi = \frac{R_1 \operatorname{sn}(\eta(\xi_1-\xi_0), m_2) + R_2 \operatorname{cn}(\eta(\xi_1-\xi_0), m_2)}{R_3 \operatorname{sn}(\eta(\xi_1-\xi_0), m_2) + R_4 \operatorname{cn}(\eta(\xi_1-\xi_0), m_2)}\,, \tag{37}
$$

where

$$
\eta = \frac{s_2\sqrt{\left(R_3^2+R_4^2\right)\left(f_2^2 R_3^2 + R_4^2\right)}}{R_3^2 + R_4^2}\,. \tag{38}
$$

Equation (37) is a double-periodic elliptic function solution.

Case 3. When $R_4 < 0$ and $R_2 R_3 \geq 0$, $Q(\phi)$ is represented as follows:

$$
Q(\phi) = (\phi-\mu)(\phi-\beta)\left[(\phi-r)^2 + o^2\right]\,, \qquad (\mu+\beta+r=0)\,, \tag{39}
$$

where $\mu > \beta$ and $o > 0$.

We obtain the following transformation:

$$
\phi = \frac{R_1 \cos\theta + R_2}{R_3 \cos\theta + R_4}\,, \tag{40}
$$

where

$$\begin{aligned} R_1 &= \frac{1}{2}(\mu+\beta)R_3 - \frac{1}{2}(\mu-\beta)R_4\,, \\ R_2 &= \frac{1}{2}(\mu+\beta)R_4 - \frac{1}{2}(\mu-\beta)R_3\,, \\ R_3 &= \mu - r - \frac{o}{f_2}\,, \\ R_4 &= \mu - r - o f_2\,, \\ e_2 &= \frac{o^2+(\mu-r)(\beta-r)}{o(\mu-\beta)}\,, \\ f_2 &= e_2 \pm \sqrt{e_2^2+1}\,, \end{aligned} \tag{41}$$

which yields the following equation when $f_2 > 0$:

$$\begin{aligned} \pm(\xi-\xi_0) &= \int \frac{\mathrm{d}q}{\sqrt{\pm(\phi-\mu)(\phi-\beta)\left((\phi-r)^2+o^2\right)}} \\ &= \frac{2f_2 m_2}{\sqrt{\mp 2 l f_2(\mu-\beta)}} \int \frac{\mathrm{d}\phi}{\sqrt{r - m_2^2\sin^2\theta}}\,, \end{aligned} \tag{42}$$

where $m_2^2 = \frac{1}{1+f_2^2}$. Thus,

$$\cos\theta = \mathrm{cn}\left(\frac{\sqrt{\mp 2 m_2 f_2(\mu-\beta)}}{2 f_2 m_2}(\xi_1-\xi_0), m_2\right), \tag{43}$$

and we obtain the following solution:

$$\phi = \frac{R_1\,\mathrm{cn}\left(\frac{\sqrt{\mp 2 m_2 f_2(\mu-\beta)}}{2 f_2 m_2}(\xi_1-\xi_0), m_2\right) + R_2}{R_3\,\mathrm{cn}\left(\frac{\sqrt{\mp 2 m_2 f_2(\mu-\beta)}}{2 f_2 m_2}(\xi_1-\xi_0), m_2\right) + R_4}\,, \tag{44}$$

where Eq. (44) is a double-periodic elliptic function solution.

Case 4. When $R_4 > 0$, $R_2 > 0$, and $R_3 > 0$, we obtain the following equation:

$$Q(\phi) = (\phi-\mu_1)(\phi-\mu_2)(\phi-\mu_3)(\phi-\mu_4)\,, \qquad (\mu_1+\mu_2+\mu_3+\mu_4 = 0)\,, \tag{45}$$

where $\mu_1 > \mu_2 > \mu_3 > \mu_4$, using the following transformations:

$$\phi = \frac{\mu_2(\mu_1-\mu_4)\sin^2\theta - \mu_1(\mu_2-\mu_4)}{(\mu_1-\mu_4)\sin^2\theta - (\mu_2-\mu_4)}\,, \qquad (\phi > \mu_1 \text{ or } \phi < \mu_4)\,, \tag{46}$$

or

$$\phi = \frac{\mu_4(\mu_2-\mu_3)\sin^2\theta - \mu_3(\mu_2-\mu_4)}{(\mu_2-\mu_3)\sin^2\theta - (\mu_2-\mu_4)}\,, \qquad (\mu_3 < \phi < \mu_2)\,, \tag{47}$$

we obtain the following equation:

$$\begin{aligned} \xi_1 - \xi_0 &= \int \frac{\mathrm{d}\phi}{\sqrt{(\phi-\mu_1)(\phi-\mu_2)(\phi-\mu_3)(\phi-\mu_4)}} \\ &= \frac{2}{\sqrt{(\mu_1-\mu_3)(\mu_2-\mu_4)}} \int \frac{\mathrm{d}\theta}{\sqrt{1-m^2\sin^2\theta}}\,, \end{aligned} \tag{48}$$

where $m^2 = \frac{(\mu_1-\mu_4)(\mu_2-\mu_3)}{(\mu_1-\mu_3)(\mu_2-\mu_4)}$. Then we have

$$\phi = \frac{\mu_2(\mu_1-\mu_4)\,\mathrm{sn}^2\left(\frac{\sqrt{(\mu_1-\mu_3)(\mu_2-\mu_4)}}{2}(\xi_1-\xi_0), m\right) - \mu_1(\mu_2-\mu_4)}{(\mu_1-\mu_4)\,\mathrm{sn}^2\left(\frac{\sqrt{(\mu_1-\mu_3)(\mu_2-\mu_4)}}{2}(\xi_1-\xi_0), m\right) - (\mu_2-\mu_4)}\,, \tag{49}$$

and

$$\phi = \frac{\mu_4(\mu_2-\mu_3)\,\mathrm{sn}^2\left(\frac{\sqrt{(\mu_1-\mu_3)(\mu_2-\mu_4)}}{2}(\xi_1-\xi_0), m\right) - \mu_3(\mu_2-\mu_4)}{(\mu_2-\mu_3)\,\mathrm{sn}^2\left(\frac{\sqrt{(\mu_1-\mu_3)(\mu_2-\mu_4)}}{2}(\xi_1-\xi_0), m\right) - (\mu_2-\mu_4)}\,. \tag{50}$$

Equations (49) and (50) are two double-periodic elliptic function solutions.

According to the seven cases mentioned above, the original equation has periodic solutions and solitary wave solutions. Specifically, the solitary wave solutions consist of kink, antikink, and singular solitary wave solutions. Therefore, the conclusions drawn in the previous section are validated.

To further enrich our findings, the following cases explore rational function solutions.

4.3. Rational function solutions

Case 1. When $R_4 = 0$, $R_3 = 0$, and $R_2 = 0$, $Q(\phi)$ is denoted as follows:

$$Q(\phi) = \phi^4\,. \tag{51}$$

Thus, we can obtain the following equations:

$$\pm(\xi_1 - \xi_0) = \int \frac{\mathrm{d}\phi}{\phi^2} = -\phi^{-1}\,, \tag{52}$$

and

$$\phi = \mp \frac{1}{\xi_1 - \xi_0} \,. \tag{53}$$

Equation (53) is a rational function solution.

Case 2. When $R_4 = 0$, $R_3 = 0$, $R_2 > 0$, $Z_2 = 0$, we have

$$Q(\phi) = (\phi - r)^3 (\phi - o) \,, \qquad (o + 3s = 0) \,. \tag{54}$$

We obtain the following equation:

$$\pm(\xi_1 - \xi_0) = \int \frac{\mathrm{d}\phi}{(\phi - r)\sqrt{(\phi - r)(\phi - o)}} = \frac{2}{o - r}\sqrt{\frac{\phi - o}{\phi - r}} \,. \tag{55}$$

Therefore, we obtain the following solutions:

$$\phi = \frac{4(r - o)}{(o - r)^2 (\xi_1 - \xi_0)^2 - 4} + r \,. \tag{56}$$

In this case, equation (56) represents a rational function solution that is distinct from the one presented in Case 1.

Case 3. For $R_4 = 0$, $R_3 = 0$, $R_2 > 0$, and $Z_2 = 0$, we obtain

$$Q(\varphi) = (\varphi - r)^3 (\varphi - o) \,, \qquad (o + 3s = 0) \,, \tag{57}$$

which yields the following equation:

$$\pm(\xi_1 - \xi_0) = \int \frac{\mathrm{d}\varphi}{(\varphi - r)\sqrt{(\varphi - r)(\varphi - o)}} = \frac{2}{o - r}\sqrt{\frac{\varphi - o}{\varphi - r}} \,. \tag{58}$$

Thus, we get

$$\varphi = \frac{4(r - o)}{(o - r)^2 (\xi_1 - \xi_0)^2 - 4} + r \,. \tag{59}$$

Equation (59) is also a rational function solution. Compared with existing studies, Wang *et al.* [41] used the trial equation method to obtain dark and single solitons and Yildirim *et al.* [42] applied four integration schemes to analyze optical solitons and straddled stationary solitons. However, this study presents for the first time all traveling wave solutions to Eq. (1) are presented.

To investigate the nature of the obtained solutions, graphical simulations are conducted. Equation (21) is selected to represent the solitary wave solutions, whereas Eq. (44) represents the elliptic periodic solutions. The corresponding parameters are set as $o = 1$, $r = -1$, $\xi_0 = 0$, $v = 5$ for Eq. (21) and $o = 3$, $\mu = 1$, $\beta = -1$, $r = 0$, $\xi_0 = 0$, $f_2 = 2$, $m_2 = \frac{\sqrt{5}}{5}$ for Eq. (44). Graphical simulations are performed on the soliton and periodic solutions, resulting in Figs. 5 and 6, which are generated by using the MATLAB software.

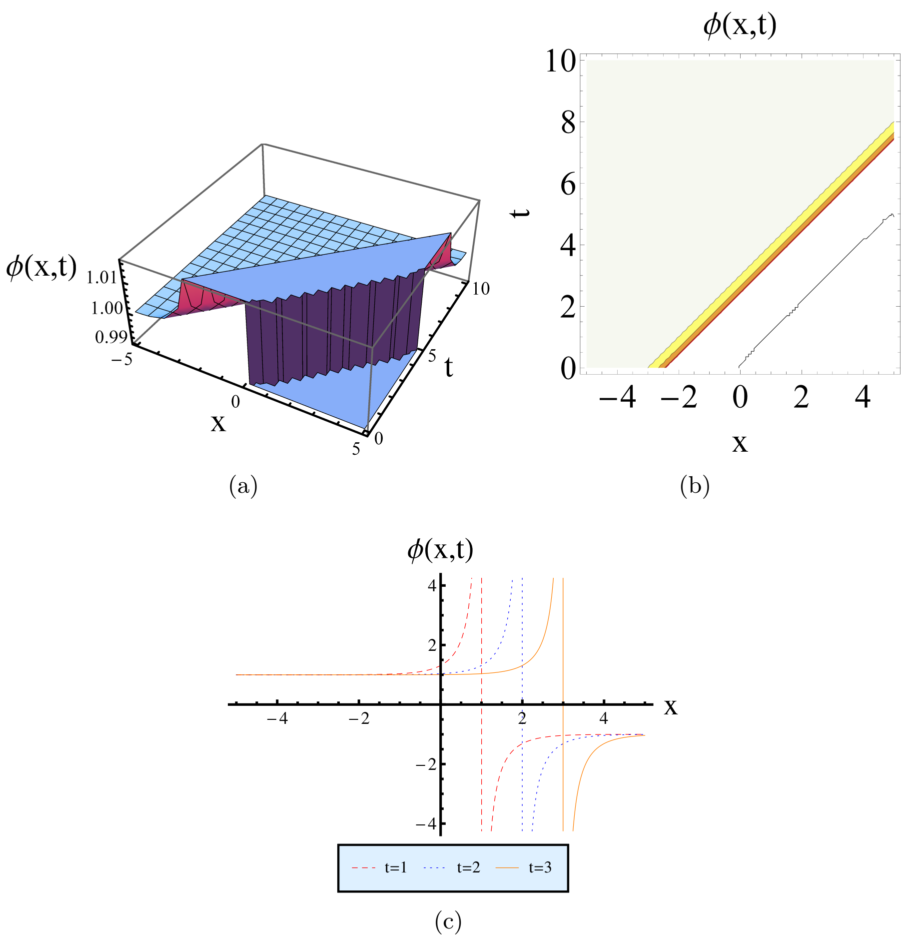

Fig. 5. Graphical simulations of Eq. (21): (a) 3D graph; (b) contour graph; (c) 2D graph.

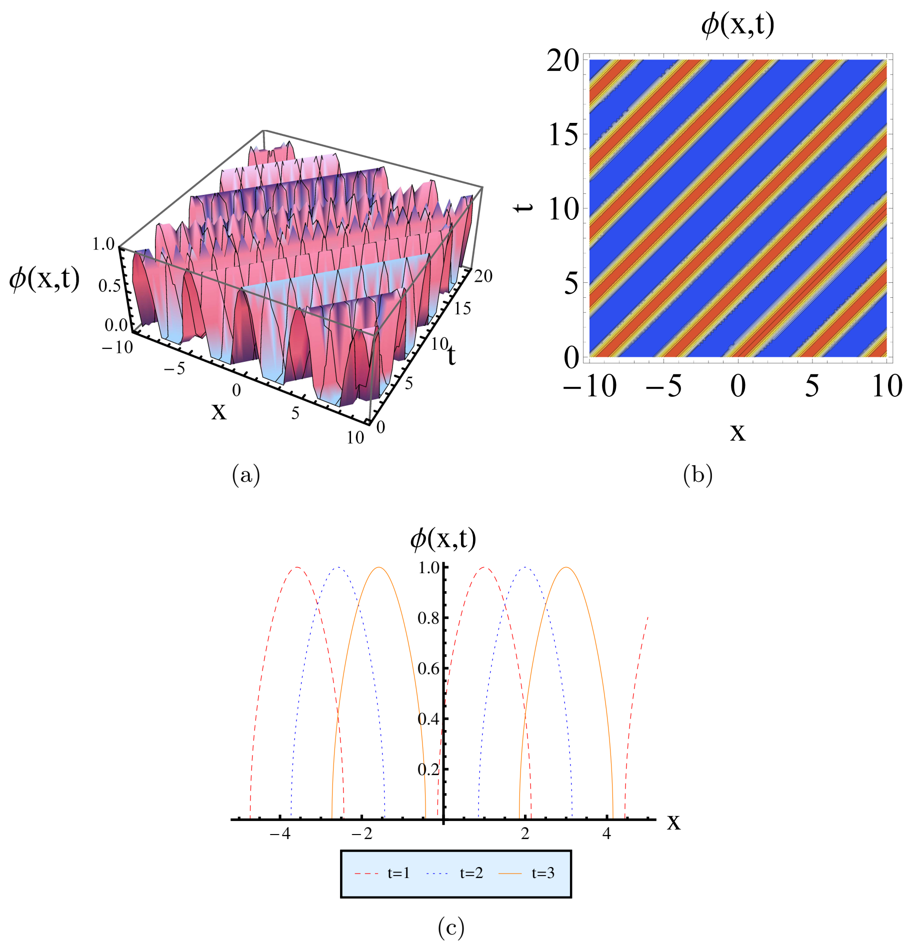

Fig. 6. Graphical simulations of Eq. (44): (a) 3D graph; (b) contour graph; (c) 2D graph.

According to Figs. 5 and 6, the physical phenomena can be intuitively observed, revealing significant differences between the distributions of soliton and periodic solutions. Figures 5 (a) and 5 (b) show that the solution distributions are relatively regular and conform to the characteristics of periodic solutions. In Fig. 5 (c), the peak value of the solution remains constant over time, indicating that the solution has the characteristic of convergence. From Fig. 6, it can be concluded that the concatenation model has solitary wave solutions, thereby verifying the accuracy of the obtained solutions.

5. Chaotic behaviors

From the above discussion, it is evident that the traveling wave system of the original model does not exhibit chaotic behavior. However, in this section, we prove that by introducing proper external perturbation terms, chaotic behaviors emerge. To verify this, we provide the corresponding phase diagram and calculate the largest Lyapunov exponent (LLE). First, the original dynamic system is rewritten in the following form:

$$\begin{aligned} \phi' &= \psi\,, \\ \psi' &= 2\left(\phi^3 + b_2\varphi + b_1\right) + \eta(\zeta)\,, \end{aligned} \tag{60}$$

where $\eta(\zeta)$ is the external perturbation.

Case 1. When $\eta(\zeta) = -(0.8)\cos(0.015\zeta)$, the corresponding figures are shown in Fig. 7. From Fig. 7 (a), it is evident that this system exhibits the chaotic phenomenon, and the positive LLE corresponding to the coefficients verifies this conclusion.

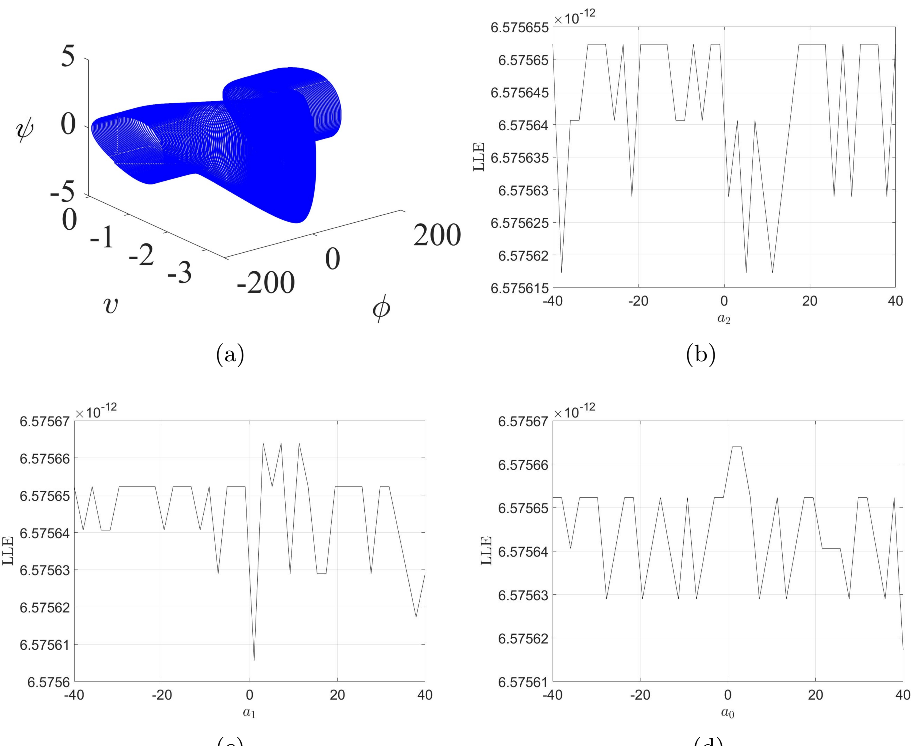

Fig. 7. Diagram of Eq. (60) when $a_2 = -0.75$, $a_1 = -0.125$: (a) phase graph; (b) LLE for a_2; (c) LLE for a_1; (d) LLE for a_0.

Case 2. When $\eta(\zeta) = -200\exp(-0.035t^2)$, the corresponding figures are shown in Fig. 8. It can be seen that under different perturbation terms, the chaotic behaviors of the original system vary. However, the exact mechanisms by which external terms affect the system or which specific terms lead to chaotic behavior remain unknown. We leave this as an open problem for future investigation.

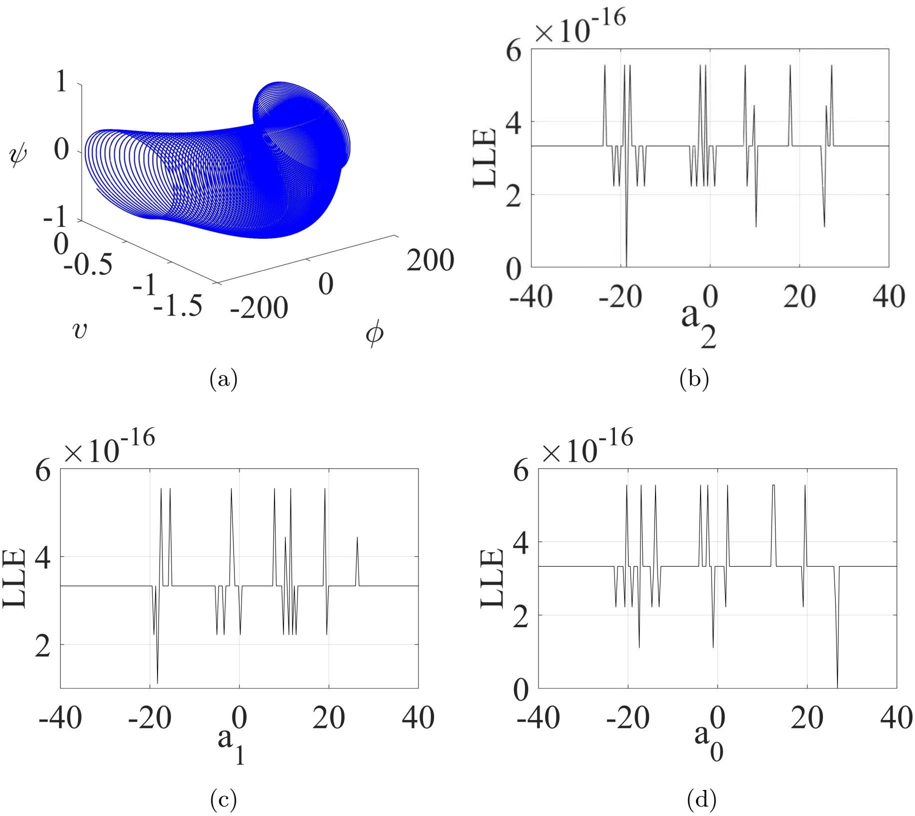

Fig. 8. Diagram of Eq. (60) when $a = -0.25, b = -0.125$: (a) phase graph; (b) LLE for a_2; (c) LLE for a_1; (d) LLE for a_0.

6. Conclusions

In this paper, the concatenation model with the power-law nonlinearity is comprehensively studied. The original equation is transformed into a dynamic system, followed by a qualitative analysis. By applying the bifurcation theory, the system's qualitative properties including global phase portraits and equilibrium points are revealed. The existence of periodic and soliton solutions is proven, and to verify this conclusion, the classification of traveling wave solutions is constructed, including several new solutions initially introduced in this paper. The obtained solutions of the concatenation model are intuitively analyzed using graphical simulations, showcasing their distribution and convergence characteristics. This means more interesting structures in quantum optics may be discovered from the results obtained. In addition, chaotic behaviors are identified by introducing specific external terms. This study provides a new perspective on the concatenation model, presenting novel results, such as elliptic function double-periodic solutions and chaotic behaviors, for the first time. This detailed exploration of the concatenation model with the power-law nonlinearity contributes to a broader understanding of nonlinear dynamics in complex systems and has profound implications for optical communication and other nonlinear optical applications. And this is the first time that the link between the chaotic behaviors and the concatenation model with power-law nonlinearity is presented, which may also be helpful in quantum chaotic theory.

This research was funded by the Heilongjiang Postdoctoral Foundation (No. LBH-Z22043,LBH-Z20101), Heilongjiang Province' Basic Research Support Program for Excellent Young Teachers (No. YQJH2023086), Northeast Petroleum University Talent Introduction and Research Initiation Funding Project (No. 2021KQ18,2019KQ54), Northeast Petroleum University National Natural Science Foundation Cultivation Fund (No. 2023GPL-14), and National Natural Science Foundation of China (No. 52104065).

REFERENCES

[1] L. Tang, A. Biswas, Y. Yildirim, A.A. Alghamdi, «Bifurcation analysis and optical solitons for the concatenation model», *Phys. Lett. A* **480**, 128943 (2023).

[2] L. Tang, «Optical solitons perturbation for the concatenation system with power law nonlinearity», *J. Opt.* **54**, 789 (2025).

[3] L. Tang *et al.*, «Bifurcation analysis and optical solitons for the dispersive concatenation model», *Ukr. J. Phys. Opt.* **25**, 03031 (2024).

[4] Y. Yildirim, A. Biswas, A.A. Asiri, «A full spectrum of optical solitons for the concatenation model», *Nonlinear Dyn.* **112**, 601 (2024).

[5] A. Biswas *et al.*, «Optical solitons for the concatenation model with power-law nonlinearity: undetermined coefficients», *Ukr. J. Phys. Opt.* **24**, 185 (2023).

[6] X.N. Li, G.M. Wei, Y.Q. Liang, «Painlevé analysis and new analytic solutions for variable-coefficient Kadomtsev–Petviashvili equation with symbolic computation», *Appl. Math. Comput.* **216**, 3568 (2010).

[7] A.D. Jagtap, E. Kharazmi, G.E. Karniadakis, «Conservative physics-informed neural networks on discrete domains for conservation laws: Applications to forward and inverse problems», *Comput. Methods Appl. Mech. Eng.* **365**, 113028 (2020).

[8] O. González-Gaxiola, A. Biswas, C.J. Ruiz, A. Asiri, «Bright and dark optical solitons for the concatenation model by the Laplace–Adomian decomposition scheme», *Ukr. J. Phys. Opt.* **24**, 222 (2023).

[9] S. Ahmed, A.H.S. Shokhan, M.R. Ahmed, «Laplace Adomian and Laplace Modified Adomian Decomposition Methods for Solving Nonlinear Integro-Fractional Differential Equations of the Volterra–Hammerstein Type», *Iraqi J. Sci.* **60**, 2207 (2019).

[10] N. Sucu, M. Ekici, A. Biswas, «Stationary optical solitons with nonlinear chromatic dispersion and generalized temporal evolution by extended trial function approach», *Chaos, Solitons Fractals* **147**, 110971 (2021).

[11] A.H. Arnous *et al.*, «Optical solitons and conservation laws for the concatenation model: Power-law nonlinearity», *Ain Shams Eng. J.* **15**, 102381 (2024).

[12] L. Tang, «Qualitative analysis, traveling wave solutions and chaotic behavior for the perturbed Schrödinger–Hirota equation with cubic–quintic–septic law of self-phase modulation», *Mod. Phys. Lett. B* (2025).

[13] L. Tang, «Qualitative Analysis, Chaotic Behavior and Optical Solitons Perturbation for the Coupled Fokas–Lenells System in Birefringent Fibers», *Qual. Theory Dyn. Syst.* **24**, 59 (2025).

[14] Y. Kai, Y. Li, «Wave structures and the chaotic behaviors of the cubic–quartic nonlinear Schrödinger equation for parabolic law in birefringent fibers», *Nonlinear Dyn.* **111**, 8701 (2023).

[15] Y. Li, W. Sun, Y. Kai, «Chaotic behaviors, exotic solitons and exact solutions of a nonlinear Schrödinger-type equation», *Optik* **285**, 170963 (2023).

[16] A. Rozanova-Pierrat, «Qualitative analysis of the Khokhlov–Zabolotskaya–Kuznetsov (KZK) equation», *Math. Models Methods Appl. Sci.* **18**, 781 (2008).

[17] W. Zhang, K. Zhang, X. Li, X. Ling, «Qualitative analysis of bounded traveling wave solutions to Nagumo nerve conduction equation and its approximate oscillatory solutions», *Commun. Nonlinear Sci. Numer. Simul.* **117**, 106936 (2023).

[18] Y. He, Y. Kai, «Wave structures and its evolution modeled by variant Mikhailov–Novikov–Wang equation», *Phys. Scr.* **100**, 025232 (2025).

[19] Y. Kai, Y. Li, L. Huang, «Topological properties and wave structures of Gilson–Pickering equation», *Chaos, Solitons Fractals* **157**, 111899 (2022).

[20] J. Xing, Z. Yang, Y. Ren, «Analysis of bifurcation and chaotic behavior for the flexspline of an electromagnetic harmonic drive system with movable teeth transmission», *Appl. Math. Model.* **112**, 467 (2022).

[21] H. Rezazadeh *et al.*, «Optical soliton solutions of the generalized non-autonomous nonlinear Schrödinger equations by the new Kudryashov's method», *Results Phys.* **24**, 104179 (2021).

[22] D.S. Wang, Y. Yin, «Symmetry analysis and reductions of the two-dimensional generalized Benney system via geometric approach», *Comput. Math. Appl.* **71**, 748 (2016).

[23] M. Rosa, M.D.L.S. Bruzon, M.D.L.L. Gandarias, «Lie symmetries and conservation laws of a Fisher equation with nonlinear convection term», *Discret. Contin. Dyn. Syst. S* **8**, 1331 (2015).

[24] B. Kilic, M. Inc, «The first integral method for the time fractional Kaup–Boussinesq system with time dependent coefficient», *Appl. Math. Comput.* **254**, 70 (2015).

[25] M. Inc, B. Kilic, «The first integral method for the perturbed Wadati–Segur–Ablowitz equation with time dependent coefficient», *Kuwait J. Sci.* **43**, 84 (2016).

[26] W.X. Ma, Z. Zhu, «Solving the (3+1)-dimensional generalized KP and BKP equations by the multiple exp-function algorithm», *Appl. Math. Comput.* **218**, 11871 (2012).

[27] Rahmatullah, R. Ellahi, S.T. Mohyud-Din, U. Khan, «Exact traveling wave solutions of fractional order Boussinesq-like equations by applying exp-function method», *Results Phys.* **8**, 114 (2018).

[28] C.S. Liu, «Classification of All Single Travelling Wave Solutions to Calogero–Degasperis–Focas Equation», *Commun. Theor. Phys.* **48**, 601 (2007).

[29] C.S. Liu, «All Single Traveling Wave Solutions to (3+1)-Dimensional Nizhnok–Novikov–Veselov Equation», *Commun. Theor. Phys.* **45**, 991 (2006).

[30] C.S. Liu, «The classification of travelling wave solutions and superposition of multi-solutions to Camassa–Holm equation with dispersion», *Chinese Phys.* **16**, 1832 (2007).

[31] C.S. Liu, «Representations and Classification of Traveling Wave Solutions to sinh-Gördon Equation», *Commun. Theor. Phys.* **49**, 153 (2008).

[32] C.S. Liu, «Solution of ODE $u'' + p(u)(u')^2 + q(u) = 0$ and Applications to Classifications of All Single Travelling Wave Solutions to Some Nonlinear Mathematical Physics Equations», *Commun. Theor. Phys.* **49**, 291 (2008).

[33] C.S. Liu, «Applications of complete discrimination system for polynomial for classifications of traveling wave solutions to nonlinear differential equations», *Comput. Phys. Commun.* **181**, 317 (2010).

[34] S.Q. Chen *et al.*, «Generic layout optimization design methodology for China's loop-star natural gas field pipeline network», *Nat. Gas Ind. B* **11**, 616 (2024).

[35] S.Q. Chen *et al.*, «Abundant variant wave patterns by coupled Boussinesq–Whitham–Broer–Kaup equations», *Chin. J. Phys.* **78**, 485 (2022).

[36] Y. Liu, S.Q. Chen, L.X. Wei, B. Guan, «Exact solutions to complex Ginzburg–Landau equation», *Pramana — J. Phys.* **91**, 29 (2018),

[37] B. Guan *et al.*, «The classification of single traveling wave solutions to coupled time-fractional KdV–Drinfel'd–Sokolov–Wilson system», *Results Phys.* **13**, 102291 (2019).

[38] R. Yang, Y. Kai, «Dynamical properties, modulation instability analysis and chaotic behaviors to the nonlinear coupled Schrödinger equation in fiber Bragg gratings», *Mod. Phys. Lett. B* **38**, 2350239 (2024).

[39] X. Zhuang, Y. Yu, A. Chen, «A combined forecasting method for intermittent demand using the automotive aftermarket data», *Data Sci. Manag.* **5**, 43 (2022).

[40] Y. Kai, S.Q. Chen, K. Zhang, Z. Yin, «A study of the shallow water waves with some Boussinesq-type equations», *Waves Random Complex Media* **34**, 1251 (2024).

[41] M.-Y. Wang *et al.*, «Optical solitons for a concatenation model by trial equation approach», *Electronics* **12**, 19 (2022).

[42] Y. Yildirim, A. Biswas, L. Moraru, A.A. Alghamdi, «Quiescent optical solitons for the concatenation model with nonlinear chromatic dispersion», *Mathematics* **11**, 1709 (2023).